







Probing the building blocks of galaxies: Sub-galactic scaling relations between X-ray luminosity, SFR and stellar mass

K. Kouroumpatzakis^{1,2}, A. Zezas^{1,2,3}, P. H. Sell^{1,2}, P. Bonfini^{1,2},
M. L. N. Ashby³ and S. P. Willner³

¹Department of Physics, University of Crete, GR-70013 Heraklion, Greece
email: kkouroub@physics.uoc.gr

²Institute of Astrophysics, FORTH, GR-71110 Heraklion, Greece

³Center for Astrophysics | Harvard & Smithsonian, Cambridge, MA

Abstract. It is well known that X-ray luminosity (L_X) originating from high mass X-ray binaries (HMXBs) is tightly correlated with the host galaxy's star formation rate (SFR). We explore this connection using a sample representative of the star-formation activity in the local Universe (Star-Formation Reference Survey; SFRS) along with a comprehensive set of star-formation (radio, FIR, $24\mu\text{m}$, $8\mu\text{m}$, $\text{H}\alpha$, UV, SED fitting) and stellar mass (K-band, $3.6\mu\text{m}$, SED fitting) indicators, and Chandra observations. We investigate the L_X – SFR and L_X – stellar mass (M_*) scaling relations down to sub-galactic scales of $\sim 1\text{ kpc}^2$. This way we extend these relations to extremely low SFR ($\sim 10^{-6}\text{ M}_\odot \cdot \text{yr}^{-1}$) and M_* ($\sim 10^4\text{ M}_\odot$). We also quantify their scatter and their dependence on the age of the local stellar populations as inferred from the different age sensitive SFR indicators. These results are particularly important for setting the benchmark for the formation of X-ray binaries in vigorous, but low SFR objects such as galaxies in the early Universe.

Keywords. galaxies:star formation – X-rays: galaxies – X-rays:binaries

1. Introduction

Various star-formation rate (SFR) indicators (e.g. UV, ionization emission lines, polycyclic aromatic hydrocarbons (PAHs), IR, radio) are used in order to trace recent and on-going SF. These different SFR indicators are probing different mechanisms associated to young stars (e.g. UV emission from the photospheres of the massive young stars, emission from the ionized gas that surrounds them, emission from dust absorbed UV, that is thermally re-emitted in the IR light, etc.). As a result, the integrated emission they trace corresponds to different stellar populations and therefore each indicator probes different timescales of star-formation. Among the SFR tracers, it is the emission from the ionized gas that is the most sensitive to the youngest stellar populations, with little contamination from older stars (e.g. [Murphy *et al.* 2011](#); [Boquien *et al.* 2014](#); [Cervino *et al.* 2016](#)).

In the spectral range of the X-rays it is already known that emission generated by X-ray binaries is tightly correlated with SFR and stellar mass. The integrated X-ray luminosity of low mass X-ray binaries (LMXBs) is correlated with the stellar mass (e.g. [Gilfanov, 2004](#)) and that of high mass X-ray binaries (HMXBs) with SFR (e.g. [Mineo *et al.* 2012](#)). Theoretical models show that the bulk of the XRB emission is produced by the HMXBs in short timescales ($\sim 10\text{ Myr}$; e.g. [Fragos *et al.* 2013](#)), while there is

almost constant X-ray output per unit stellar mass by the long-lived LMXBs that are active through longer times (several Gyr). Therefore correlating the HMXBs with the SFR indicators that probe stellar populations of similar ages (e.g. H_α) is important in order to constrain XRB population synthesis models, explore the cosmological evolution of compact objects, and investigate the effect of HMXBs in galaxy evolution through their effect in preheating the IGM.

In this work we address these correlations both in integrated galaxy emission (Sell *et al.* 2019) and also in sub-galactic scales (down to 1 kpc^2) in order to constrain the correlation in the regime of extremely low SFR ($\sim 10^{-6} \text{ M}_\odot \text{ yr}^{-1}$), M_\star ($\sim 10^4 \text{ M}_\odot$), and sSFR (10^{-13} yr^{-1}).

2. Sample and results

Our sample is based on the Star Formation Reference Survey (SFRS; Ashby *et al.* 2011). SFRS is comprised by 369 galaxies, that represent all modes of SF in the local Universe. They cover the 3D space of three fundamental characteristics of galaxies: the SFR, indicated by the $60 \mu\text{m}$ luminosity; the specific SFR (sSFR), indicated by the $K_s - F_{60}$ (mag) color; and the dust temperature, indicated by the FIR (F_{100}/F_{60}) flux ratio. The SFRS also benefits from a panchromatic coverage of the electromagnetic spectrum, from radio wavelengths up to the X-rays, including spectroscopic emission line nuclear classification of the galaxies (Maragkoudakis *et al.* 2017) and H_α imaging.

The sample used for this work consists of 14 star-forming (non-AGN) SFRS galaxies (NGC5879, NGC3353, UGC5720, NGC4194, NGC5691, NGC6090, NGC5474, NGC5585, MCG632070, NGC3245, NGC5584, NGC3656, UGC9618, and NGC5204) that have *Chandra* data of adequate quality to study the x-ray emission and stellar populations in 1 kpc^2 scales. The integrated emission of the sample galaxies spans ~ 4 dex in the SFR and ~ 3 dex in sSFR. In sub-galactic scales these ranges become ~ 6 dex and ~ 5 dex in SFR and sSFR respectively.

The integrated X-ray luminosity has been measured through spectral fitting of the *Chandra* spectra with the use of the *CIAO* and *Sherpa* tools, while statistically accounting for background AGN contamination. In order to measure XRBs emission, and avoid any hot gas contamination, we account the emission attributed only to the power law component of the spectral fits. The details of the spectral analysis and corresponding results are presented in Sell *et al.* 2019. Fig. 1 show the $L_X - \text{SFR}$ correlations from this work based on different SFR indicators. In this correlation, as well as in the $L_X/\text{SFR} - \text{sSFR}$ correlation, we find significant differences, both in slope and intercept, depending on the used SFR indicators. Similar differences are seen in the scatter of these correlations. We attribute these variations on the different age and attenuation sensitivity of each SFR indicator.

For the sub-galactic analysis we apply grids of 1×1 , 2×2 , and $3 \times 3 \text{ kpc}^2$ on the IRAC $3.6 \mu\text{m}$ images (used to measure the stellar mass), the H_α , IRAC $8 \mu\text{m}$, MIPS $24 \mu\text{m}$ (used to measure the SFR), and the *Chandra* images in the soft ($0.5 - 2.0 \text{ keV}$), the hard ($2.0 - 8.0 \text{ keV}$), and the total ($0.5 - 8.0 \text{ keV}$) bands. From these grids we generate SFR, sSFR, and X-ray luminosity maps (Fig. 2) which we use to correlate these parameters in each sub-galactic region.

In order to infer the X-ray luminosity of each tile we calculate the posterior probability distribution of the source counts using the BEHR tool (Park *et al.* 2006). We calculate the X-ray luminosity based on the integrated spectrum of each galaxy, and the hardness ratio of each region.

With this analysis we are capable of examining the $L_X - \text{SFR}$ correlation (Fig. 3; Left) down to extremely low SFRs ($\sim 10^{-6} \text{ M}_\odot \text{ yr}^{-1}$). We see a good agreement with the established correlation (Mineo *et al.* (2014)) down to SFR $\sim 10^{-2} \text{ M}_\odot \text{ yr}^{-1}$ but we

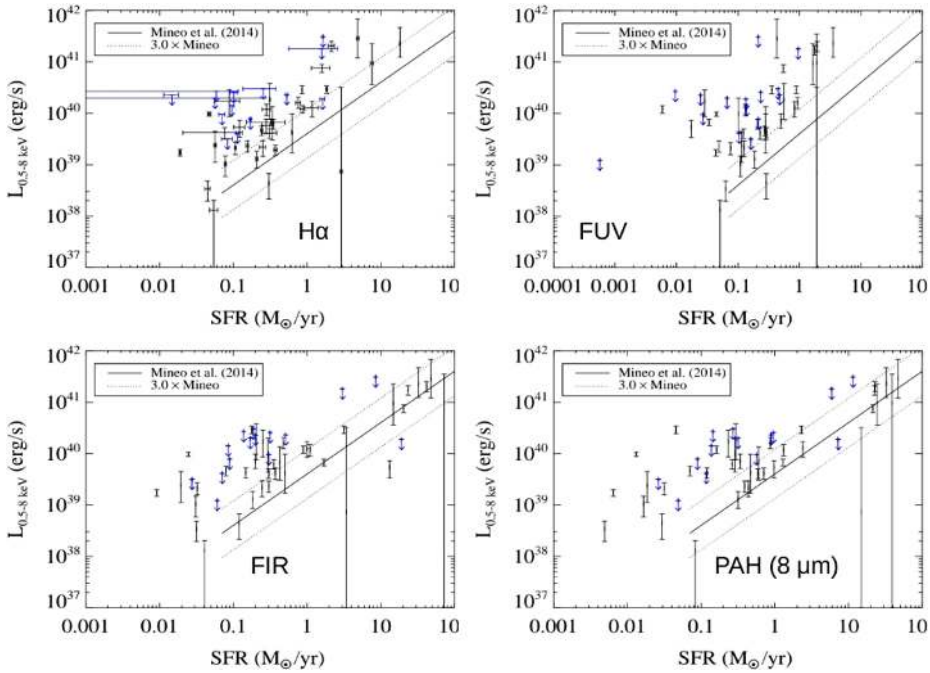


Figure 1. The $L_X - SFR$ correlations based on various SFR indicators. Clockwise from the top left we see H_α , *GALEX* FUV, PAH $8\mu m$, and FIR indicators. The black points represent detections, blue points represent upper limits and the dashed line indicates the fit of Mineo *et al.* (2014). We see a systematic excess in the H_α and FUV correlations which we attribute to attenuation. We find a better agreement with the Mineo *et al.* (2014) relation with the IR indicators.

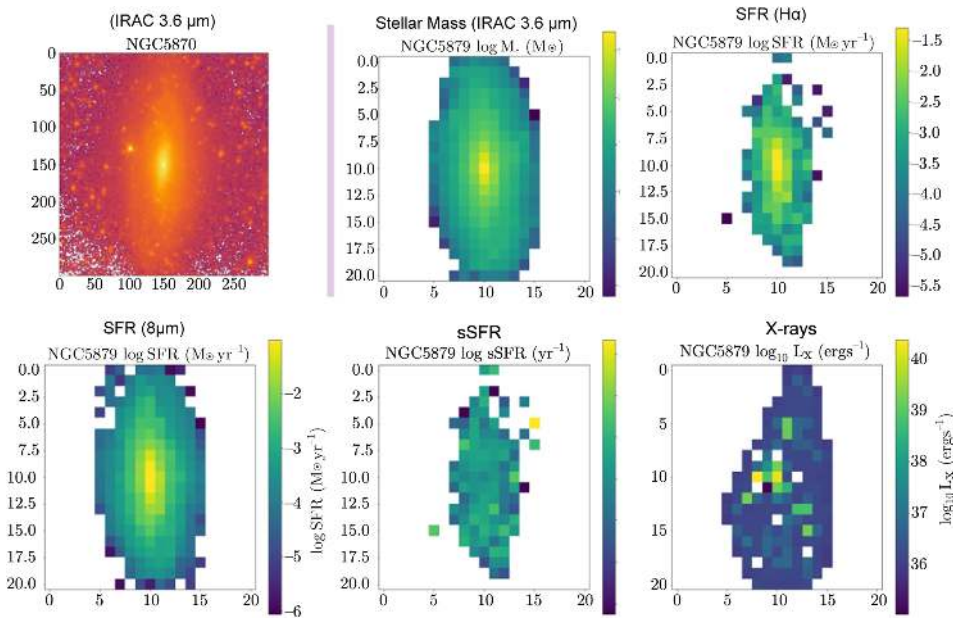


Figure 2. The 1 kpc^2 sub-galactic maps generated for galaxy NGC5879.

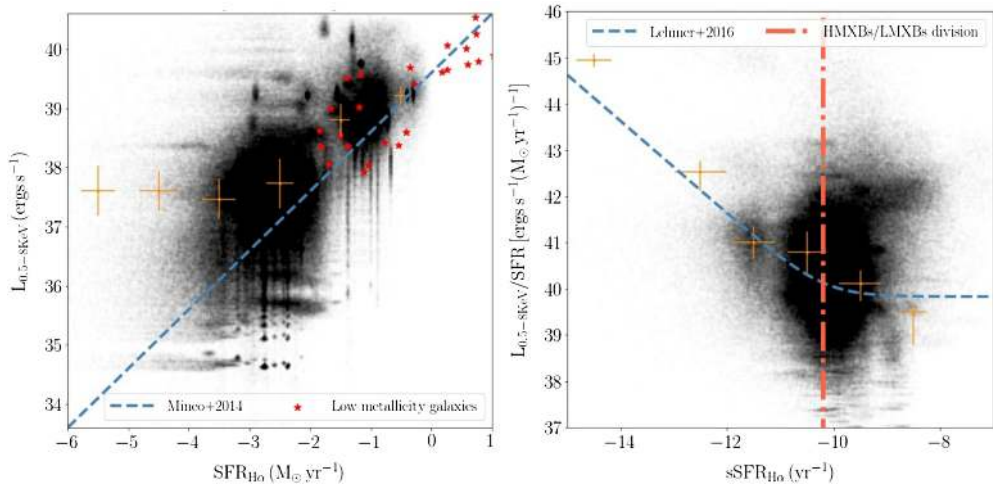


Figure 3. **Left:** The combined $L_X - SFR$ correlation in log space for all the tiles of the sample galaxies. Each tile is represented by sampling 1000 draws of the X-ray luminosity and SFR distributions, seen as the black density plot in the background. The dark orange points represent the modes and the 68% percentiles of the L_X and SFR of all the tiles in 1 dex SFR bins. The blue dashed line indicates the Mineo *et al.* (2014) fit, and the red stars represent the low metallicity galaxies from Douna *et al.* 2015. **Right:** Similarly, but showing the $L_X/SFR - SFR$ correlation. The dark orange points represent the modes and the 68% percentiles of the L_X/SFR and sSFR of all the tiles in 1 dex sSFR bins. The blue dashed line indicates the Lehmer *et al.* (2016) fit and the red dashed-dotted line indicates the division where the LMXB (left) and the HMXB (right) populations dominate.

find an excess of X-ray luminosity in lower SFRs. Similarly we examine the $L_X/SFR - sSFR$ correlation (Fig. 3; Right), where we find an exceptional agreement with the fit of Lehmer *et al.* (2016), while extending the correlation in lower values of sSFR. We also explore these correlations with other SFR indicators (PAH $8\mu m$, $24\mu m$ continuum) and in different physical scales (1×1 , 2×2 , and $3 \times 3 kpc^2$) and we still find the same behavior in both correlations.

3. Conclusions

Our results are summarized in the following points:

- We find variations in the $L_X - SFR$ correlations depending on the different SFR indicator. We interpret this as the result of the different sensitivity of each indicator in stellar population age and attenuation.
- We find that the $L_X - SFR$ correlations hold down to $SFR \sim 10^{-2} M_{\odot} yr^{-1}$ and we find an excess of X-ray luminosity in the extremely low SFR regime.
- We find similar scatter in the $L_X - SFR$ correlation between the dwarf galaxies and the sub-galactic regions which is increasing in the low SFR regime.
- We find exceptional agreement on the $L_X/SFR - sSFR$ correlation with Lehmer *et al.* (2016), while extending this correlation to lower values of sSFR. This is also an indication that the X-ray luminosity excess in the low SFR regime is due to an underlying LMXBs emission.
- With this work we will be able to quantify the magnitude of the scatter with regard to the physical scales, and measure the stochasticity in the $L_X - SFR$ correlation introduced by the different SF histories of the individual galaxies.

References

- Ashby, M., Mahajan, S., Smith, H. A., Willner, S. P., Fazio, G. G., Raychaudhury, S., Zezas, A., Barmby, P., *et al.* 2011, *PASP*, 123, 907
- Boquien, M., Buat, V., Perret, V., *et al.* 2014, *A&A*, 571, A72
- Cervino, M., Bongiovanni, A., Hidalgo, S., *et al.* 2016, *A&A*, 589, A108
- Douna, V. M., Pellizza, L. J., Mirabel, I. F., Pedrosa, S. E., *et al.* 2015, *A&A*, 579, A44
- Fragos, T., Lehmer, B., Tremmel, M., Tzanavaris, P., Basu-Zych, A., Belczynski, K., Hornschemeier, A., Jenkins, L., *et al.* 2013, *AJ*, 764, 1
- Gilfanov, M. 2004, *MNRAS*, 349, 1
- Lehmer, B. D., Basu-Zych, A. R., Mineo, S., Brandt, W. N., Eufrazio, R. T., Fragos, T., Hornschemeier, A. E., Luo, B., *et al.* 2016, *AJ*, 825, 1
- Maragkoudakis, A., Zezas, A., Ashby, M. L. N., Willner, S. P., *et al.* 2017, *MNRAS*, 475, 2
- Mineo, S., Gilfanov, M., Sunyaev, R., *et al.* 2012, *AJ*, 737, 2
- Mineo, S., Gilfanov, M., Lehmer, B. D., Morrison, G. E., Sunyaev, R., *et al.* 2014, *MNRAS*, 437, 2
- Murphy, E. J., Condon, J. J., Schinnerer, E., Kennicutt, R. C., Calzetti, D., Armus, L., Helou, G., Turner, J. L., *et al.* 2011, *MNRAS*, 419, 3
- Park, T., Kashyap, V. L., Siemiginowska, A., van Dyk, D. A., Zezas, A., Heinke, C., Wargelin, B. J., *et al.* 2006, *AJ*, 652, 1
- Sell, P., Zezas, A., Kouroumpatzakis, K., Bonfini P., Ashby, M., Willner S., *et al.* 2019, *In preparation*

Discussion

DANIEL SCHAEERER: To include X-ray emission in evolutionary synthesis models and to test them we need observational constraints and the X-ray emissions of simple populations at different ages. Are there such constraints for your observations or others?

KONSTANTINOS KOUROUMPAZAKIS: Our analysis can help constrain the detected populations of LMXBs and HMXBs in different conditions of star-formation (low, high) and in regard with the time scales of the observed SFR in sub galactic regions of galaxies. Therefore we will be able to constrain what should be expected by the population synthesis models.

DAVID ROSARIO: Looking at low sSFR systems where HMXBs are not important, should AGN boost the X-ray emission or contaminate that from LMXBs?

KONSTANTINOS KOUROUMPAZAKIS: We have tried to account for any possible contamination of AGN contribution in the L_x measured in our analysis. We statistically excluded it in the X-ray fits, and also excluded the sub-galactic nuclear regions for those that it is known (by spectral classification) that host an AGN.

THEMIYA NANAYANNARA: There is a known problem of lack of FUV photons in SSPs to explain observed spectra. This is related to He+ ionizing photons. Can we and how can HMXBs can be included to the SSPs to solve this problem?

KONSTANTINOS KOUROUMPAZAKIS: Constraining the SFR limit where the underlying LMXB L_x contribution is higher than the HMXB L_x , will help constrain the binary stellar evolutionary models and maybe indicate the lack of the UV photons in SSPs.

TOMO GOTO: How strong is an SFR indicator in $L_x < 10^{38}$? Can you correlate M_* to do? In principal should be able to solve.

KONSTANTINOS KOUROUMPAZAKIS: When we observe high values of L_x , we know that the bulk of the emission is attributed to HMXBs. In the low SFR regime, due to the lack of recent star-formation, we attribute the L_x to LMXBs and therefore this L_x correlates with the M_* of the regions.